

# Entity Alignment with Unlabeled Dangling Cases

Hang Yin<sup>1</sup>, Dong Ding<sup>1</sup>, Liyao Xiang<sup>1</sup>, Yuheng He<sup>1</sup>, Yihan Wu<sup>1</sup>, Xinbing Wang<sup>1</sup>, Chenghu Zhou<sup>2</sup>

<sup>1</sup>Shanghai Jiao Tong University, Shanghai, China, <sup>2</sup>Chinese Academy of Sciences, Beijing, China

{yinhang\_SJTU, 18916162516, xiangliyao08, heyuheng, caracalla, xwang8}@sjtu.edu.cn  
zhouchsjtu@gmail.com

**Abstract**—We investigate the entity alignment problem with unlabeled dangling cases, meaning that there are entities in the source or target graph having no counterparts in the other, and those entities remain unlabeled. The problem arises when the source and target graphs are of different scales, and it is much cheaper to label the matchable pairs than the dangling entities. To solve the issue, we propose a novel GNN-based dangling detection and entity alignment framework. While the two tasks share the same GNN and are trained together, the detected dangling entities are removed in the alignment. Our framework is featured by a designed entity and relation attention mechanism for selective neighborhood aggregation in representation learning, as well as a positive-unlabeled learning loss for an unbiased estimation of dangling entities. Experimental results have shown that each component of our design contributes to the overall alignment performance which is comparable or superior to baselines, even if the baselines additionally have 30% of the dangling entities labeled as training data.

**Index Terms**—Knowledge Graph, Entity Alignment, Positive-Unlabeled Learning, Dangling Cases

## I. INTRODUCTION

Entity alignment (EA) seeks the entities across different knowledge graphs (KGs) that refer to the same real-world identity, such as English entity `Apple` and its French `pomme`. EA has been widely deployed in many areas such as cross-lingual translation, knowledge fusion, question-answering, web mining, etc. Conventional approaches to EA exploit a wide range of discriminative entity features including names, descriptive annotations, and relational structures [1]–[3] to link different entities. More recently, embedding-based methods have been proposed to represent the entities by low-dimensional embeddings and capture their similarity in the embedding space. The embedding-based approaches can also be divided into translation-based and graph neural network (GNN)-based, depending on how the embeddings are generated. The former methods [4]–[6] employ the translational models to learn entity embeddings given entity features, whereas the latter [7]–[11] adopt GNNs for learning the graph structures.

The entities without alignment across KGs are called *dangling entities*. Let’s take the native biological KGs of Africa and America for example, the entity `zebra` will be one part of Africa’s KG but for that of America. On the contrary, the `puma` constitutes the KG of America but for that of Africa. Both entities of `zebra` and `puma` are defined as dangling entities. Most of the existing EA methods search for alignment by comparing the similarity of entity pairs. The presence of dangling entities in the candidate entity set, on the one hand,

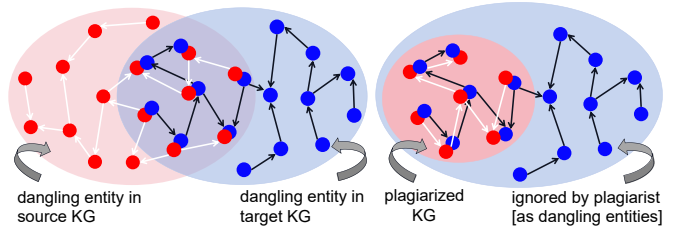


Fig. 1: Two cases of dangling entities. Left: Dangling entities are in both source and target KGs. Right: Dangling cases are merely in the target KG.

leads to more unnecessary query burden and, on the other hand, increases the possibility of getting the wrong alignment.

Despite that many works have been investigating the entity alignment problem, few are focusing on the EA with dangling cases, a problem commonly occurring in practice shown as Fig. 1. For example, one KG  $G_s$  is suspicious of misusing a part of another KG  $G_t$  without the creators’s consent. The authors of  $G_t$  would like to collect evidence of copyright violation by aligning  $G_s$  with  $G_t$ , although there may not be a one-to-one mapping between the two graphs. In general, the entities in one KG that do not have counterparts in the other KG are called dangling entities whereas the rest are matchable ones. EA with dangling entities is more challenging in that one theoretically needs to exhaust all possible mapping targets to determine whether an entity has no counterparts. Dangling entities essentially break the one-to-one mapping assumption commonly held by the current EA methods, thus rendering many methods ineffective.

Motivated by the copyright violation detection of KG, we investigate the EA problem with dangling cases, yet facing three challenges: *first*, access to the KG is restricted in realistic problem, we struggle to locate the problem in the absence of attributes. The truth is that some entity attributes in KGs is often missing or biased [12]. To be specific in copyright violation detection, the attacker might deliberately modify the corresponding attributes to mislead censorship. On the other side, EA plays a vital role in downstream KG completion for both attributes and links [13]. Over-reliance on attribute information is to put the cart before the horse. It means that EA with dangling cases needs to be done in a general setting where only graph structural information can be used. Different

from attribute or side information, the distribution of graph structure is highly non-i.i.d [14], posing a severer challenge to alignment. *Second*, a large number of dangling entities would lead to erroneous information propagating through neighborhood aggregation, negatively affecting the alignment of matchable entities. The issue is rooted in the over-smoothing problem of GNN in representing entities by aggregating all their neighborhood information. *Third*, most dangling entities are hard to label for dangling detection while it is typical to have some seed anchor pairs to initiate the alignment of other entities. This is because detecting an entity having no counterparts is much more expensive than detecting a pair of matchable entities. While it is easy to align a pair of seed nodes by querying the source entity in the target graph, it is harder to claim one entity has no matches. Hence our proposed EA task has paired entities as seeds but not any labeled dangling entities. Learning in the unlabeled-dangling-entities setting can be quite challenging, as it is hard to portray corresponding dangling consistent distribution directly from training set, requiring the model to distinguish potential dangling entities while unifying the matchable entities representation.

Given these challenges, we list related prior works in Tab. I to see how they address them. Sun et al. [15] propose three techniques based on MTransE [16] and AliNet [8] without any side information. Their methods incorporate an auxiliary learning objective pushing the embeddings of dangling entities away from those of matchable ones to distinguish the two types of nodes but require a portion of dangling and matchable entities labeled as training data. Removing the requirement for labeled dangling entity information, UED [4] and SoTead [17] propose unsupervised schemes for EA with dangling cases, but the methods rely on side information such as entity names to generate pseudo entity pairs and globally guided alignment information.

Method	Side Information	Labeled Dangling Entities
MTransE	✗	✓
AliNet	✗	✓
UED	✓	✗
SoTead	✓	✗
Our Work	✗	✗

TABLE I: Summary of EA approaches with dangling cases.

Our goal is to harness the potential of GNNs to address the three challenges. Our work is motivated by the following observations: First, we attribute the difficulty of EA with dangling cases to the ‘pollution’ caused by the abundant ambiguous dangling entities in the conventional GNN aggregation. Hence selecting which entities are used in the GNN aggregation is critical. Second, the detection of dangling entities could make some use of the annotated matchable nodes but not the dangling ones, constituting a positive-unlabeled (PU) scenario. An unbiased risk estimator should be used to fit the data distribution.

Given the observations, we propose a novel framework for EA with dangling cases on non-attributed graphs with no label information for the dangling entities. There are two intertwined phases: dangling detection and entity alignment. The two phases share one GNN backbone to learn entity representation. In the GNN, to eliminate the ‘pollution’ of dangling entities, a new entity and relation attention mechanism are designed to select useful neighborhood information for aggregation. We design two losses — a contrastive loss that disentangles the matchable entities from the dangling ones, and a positive-unlabeled learning loss that reweighs the unlabeled dangling entities in the training objective. A combination of the two losses is applied in the detection phase whereas the contrastive loss is used for the alignment phase. We identify dangling entities in the detection phase and deprive them of the right to matching. Finally, we get the remaining corresponding entities embeddings, after taking the source and target KGs as our model’s input. Then we seek the nearest neighbor entity pairs as equivalent entities in the embedding space under a given metric.

Highlights of our contributions are as follows.

- We raise a new, challenging EA problem where no dangling entities are labeled, originating from the KG copyright violation detection scene. The problem not only has practical value but also can be generalized to other non-negative-label alignment issues.
- To tackle the problem, we propose a new entity-relation attention mechanism for selective GNN aggregation and design a contrastive loss by combining the infoNCE loss and the alignment loss, which serves both entity alignment and dangling detection.
- Crucially, we introduce the positive-unlabeled learning loss into dangling detection, and further derive a tighter deviation bound than previous PU learning work. Experiments on a variety of real-world datasets have demonstrated our superior or up-to-date performance over baselines, even the dangling-aware baselines, despite that they additionally use 30% labeled dangling entities in training.

## II. PRELIMINARIES

### A. Definitions

**Definition 1: Knowledge graph (KG)** is a directed graph  $G = (E, R, T)$  comprising three distinct sets: entities  $E$ , relations  $R$ , and triples  $T \subseteq E \times R \times E$ . KG is stored in the form of triples  $\langle \text{entity}, \text{relation}, \text{entity} \rangle$ , with entities denoted by nodes and the relation between entities defined by edges.

**Definition 2 (Entity alignment):** Given source KG  $G_s = (E_s, R_s, T_s)$  and target KG  $G_t = (E_t, R_t, T_t)$ , and a set of pre-aligned anchor node pairs  $A = \{(u, v) | u \in E_s, v \in E_t, u \equiv v\}$ , where  $\equiv$  indicates equivalence, the goal of entity alignment is to identify additional pairs of potentially equivalent entities using information from  $G_s$ ,  $G_t$ , and  $A$ . This task typically assumes a one-to-one correspondence between  $E_s$  and  $E_t$ .

**Definition 3 (Entity alignment with dangling cases):** Let entities in the source and target graphs be composed of two

types of nodes:  $E_s = D_s \cup M_s, E_t = D_t \cup M_t$ , where  $D_s, D_t$  denote dangling sets that contain entities that have no counterparts, and  $M_s, M_t$  are matchable sets. A set of pre-aligned anchor node pairs are  $S = \{(u, v) | u \in M_s, v \in M_t, u \equiv v\}$ . The task seeks to discover the remaining aligned entities given  $G_s, G_t$ , and  $S$ .

### B. Transductive Learning:

Transductive learning models are trained from observed, specific (training) cases to specific (test) cases, employing both training and test information except for test labels. In contrast, inductive learning model is reasoning from observed training cases to general rules, which are then applied to the test cases. Let's get down to EA task. As KG structure is accessible through given triples, which can accurately describe the connections between entities. When we attempt to figure out entity alignment tasks, the KG structure information of the whole source and target KGs is what we could exploit, covering potentially (test) equivalent entities' relative positions. That's why we confine the problem field to transductive learning.

### C. Positive-Unlabeled Learning

Let  $X \in \mathbb{R}^d, d \in \mathbb{N}$ , and  $Y \in \{\pm 1\}$  be the input and output random variables. We also define  $p(x, y)$  to be the joint probability density of  $(X, Y)$ ,  $p_p(x) = p(x | y = +1)$ ,  $p_n(x) = p(x | y = -1)$  to be the *P (Positive) and N (Negative) marginals (a.k.a., class-conditional densities)*, and  $p_u(x)$  be the *U (Unlabeled) marginal*. The *class-prior probability* is expressed as  $\pi_p = p(y = +1)$ , assumed known throughout the paper, which can be estimated from known datasets [18].

The transductive PU learning problem setting is as follows: the positive and unlabeled data are sampled independently from  $p_p(x)$  and  $p_u(x)$  as  $\mathcal{X}_p = \{x_i^p\}_{i=1}^{n_p} \sim p_p(x)$  and  $\mathcal{X}_u = \{x_i^u\}_{i=1}^{n_u} \sim p_u(x)$ , and a classifier is trained from  $\mathcal{X}_p$  and  $\mathcal{X}_u$ , in contrast to learning a classifier telling negative samples apart from positive ones. The general assumption of the previous work is to let the unlabeled distribution be equal to the overall data distribution, i.e.,  $p_u(x) = p(x)$  since  $p_u(x)$  cannot be obtained, but the assumption hardly holds in many real-world scenarios, for example transductive learning, making methods in [18], [19] infeasible.

### D. Graph Convolutional Networks

For graph convolutional networks (GCN) [20], the embedding  $\mathbf{h}_{e_i}^{l+1}$  of node  $e_i$  at the  $l+1$ -th layer is updated iteratively by aggregating node features of the neighboring nodes  $\mathcal{N}_{e_i}$  from the prior layer:

$$\mathbf{h}_{e_i}^{l+1} = \sigma \left( \sum_{e_j \in \mathcal{N}_{e_i} \cup \{e_i\}} \alpha_{i,j} W^{l+1} \mathbf{h}_{e_j}^l \right), \quad (1)$$

where each embedding  $\mathbf{h}_{e_i}^l$  represents the  $d$ -dimensional embedding vector of  $e_i$ ,  $\alpha_{i,j}$  denotes the weight coefficient between  $e_i$  and  $e_j$ ,  $W^{l+1}$  being the transformation matrix of the  $(l+1)$ -th GNN layer, and  $\sigma$  being the activation function.

## III. RELATED WORK

In this section, we briefly review the related works on the general entity alignment and the more recent dangling entity recognition problem.

### A. Entity Alignment

Embedding-based entity alignment methods have evolved rapidly and are gradually becoming the mainstream approach of EA in recent years due to their flexibility and effectiveness [21], which aim to encode KGs into low-dimensional embedding space to capture the semantic similarities of entities [22], [23]. The embedding-based EA includes at least two approaches, one being translation-based, and the other being GNN-based. Representative translation-based models include TransE [24], which learns factual knowledge embeddings from relation triples to uncover node alignment. Based on the condition where attribute information can be accurately obtained, some others [4]–[6] initialize node embeddings with additional attributes such as texts using LSTM [25], Glove [26] or LaBSE [27], but introduce name bias [12], [28], [29] in entity alignment. Specifically, some works are based on Pretrained Language Models (PLMs) like BERT [30]. These methods neglect the structure information of KGs, locating the EA problem more over attribute semantic information. The entity representations produced by PLMs are enhanced by GRU modules [31] or RBF kernel aggregation function [32].

More recent approaches apply GNN-based models like GCN [20] and GAT [33] to capture graph structure information for entity alignment. Various GNN attention mechanisms are designed. The GCN-Align [7] utilizes the global KG structure to obtain the representation of each entity by aggregating neighborhood features. AliNet [8] proposes a gating mechanism to aggregate multi-hop neighborhood information. RREA [9] employs relational reflection to obtain relation-specific coefficients as aggregation weights. Works of [10], [11] adopt semi-supervised learning to resolve the data insufficiency problem. The former seeks the mutual nearest neighbor entity pairs as additional positive samples, while the latter generates high-quality negative samples in a similar way. Our approach is a GNN-based one and is inspired by the semi-supervised learning works to incorporate a contrastive learning loss to take full advantage of the labeled data.

### B. Dangling Entity Detection

Previous EA methods mostly assume a one-to-one correspondence between two KGs, but such an assumption does not always hold and thus leads to a performance drop in real-world cases [34]. Notably, Sun *et al.* [15] point out that when removing dangling entities, the EA model can provide a more robust alignment for the remaining entities. Their work rests upon a supervised setting, i.e., a small set of seed entity alignment and a small set of known dangling entities labeled. On this basis, MHP [35] employed more dangling information concerning high-order proximities in both training and inference. However, dangling entities are unavailable in most

real-world scenarios. The two methods mentioned above can not be applied to the problem we proposed, MHP even goes off the track of increasing dependence on labeled dangling entities.

To resolve the issue, UED [4] and SoTead [36] propose an unsupervised method for joint entity alignment and dangling entity detection. The method mines the literal semantic information to generate pseudo-entity pairs and utilizes the EA results for dangling entity detection. The approach does not require labeled dangling entities but instead entails entity attributes in their translation-based model. As it solve EA problem along with DED problem, it gathered the nearest entity pairs as matchable entities without removing dangling entities, and the unaligned entities were predicated as dangling entities. The additional unnecessary query burden due to the dangling problem isn't avoided.

Our work follows the GNN-based model for entity alignment in a more general setting where dangling entities exist. We detect the dangling entities in a setting with all assumptions, such as known dangling entities, or entity attributes, removed. By eliminating the detected dangling entities, the accuracy of our EA tasks significantly improves.

#### IV. METHODOLOGY

Fig. 2 depicts the overview of our work. Our framework comprises two GNN-based encoders sharing the same structure with separate loss functions, corresponding to two intertwined tasks — dangling entity detection and entity alignment. One of the encoders is trained end to end with MLP classifier through  $\mathcal{L}_D$  for DED. The other encoder is trained to generate embeddings in a unified feature space through  $\mathcal{L}_{EA}$ . The DED results are provided in the inference phase of EA. Then, identified dangling entities are removed for aligned pairs searching thereby improving the alignment performance.

Specifically, our GNN-based encoder is featured by: an attention calculation module that introduces a learnable weight for each entity while projecting the relation between entities for feature distinguishable; an intra-graph and a cross-graph representation learning module for a unified feature space.

Two synergetic loss functions that make up  $\mathcal{L}_D$  and  $\mathcal{L}_{EA}$  were introduced by us:  $\mathcal{L}_{\text{info}}$  loss is designed to distinguish the dangling entities from the matchable ones in a unified feature space, whereas the  $\mathcal{L}_{\text{pu}}$  loss function follows the unbiased transductive risk estimator to facilitate detection without labeled dangling entity.

##### A. Entity-Relation Attention

Real-world EA tasks often involve graphs with distortion [37]. For example, plagiarists may attentionally tamper with graph structures, or KGs undergo frequent updates [38]. Such distortion may produce many dangling entities, and those dangling entities may ‘pollute’ those of the matchable entities in conventional neighborhood aggregation.

To curb ‘pollution’ from dangling entities, we intend to perform selective neighborhood aggregation by applying different weights to different entities:

$$\mathbf{h}_{e_i}^{l+1} = \sigma \left( \sum_{e_j \in \mathcal{N}_{e_i} \cup \{e_i\}} \mathbb{1}(e_j) \alpha_{i,j} W^{l+1} \mathbf{h}_{e_j}^l \right). \quad (2)$$

The indicator function  $\mathbb{1}(e_i)$  outputs a binary value of 0 or 1 to determine whether a node should be included in neighborhood aggregation. Ideally, if the dangling entity detection is precise, we could directly apply the detection result to the value of the indicator function.

In practice, there are always a few matchable entities misclassified as dangling entities. Applying the detection results directly might remove links between matchable KG subgraphs, leading to matchable entities not aggregating adequate discriminative neighborhood features. Instead, we introduce a learnable scalar weight  $r_{e_j}$  for each  $e_i$ 's neighboring nodes  $e_j$ , thus the entity embedding can be written as

$$\mathbf{h}_{e_i}^{l+1} = \sigma \left( \sum_{e_j \in \mathcal{N}_{e_i} \cup \{e_i\}} \tanh(r_{e_j}) \alpha_{i,j} W^{l+1} \mathbf{h}_{e_j}^l \right), \quad (3)$$

where  $\tanh$  serves to normalize  $r_{e_j}$  to the range of  $[-1, 1]$ . The initialization of  $r_{e_j}$  is critical. As we found, the  $\tanh$  function changes rapidly in the region close to 0 but stays stable in the region beyond  $[-3, 3]$ . Hence we initialize the  $r_{e_j}$  to 1 to prevent gradients oscillation or near-zero gradients, which facilitates better convergence and performance.

Knowledge graphs are heterogeneous graphs containing multiple relation types, rendering the isotropic mechanism in vanilla GCN incompetent. Isotropy suggests a GNN treats each edge equally in updating the representation of each node. Intuitively, treating edges differently by extracting relation embeddings may help differentiate entities within various relational contexts. Some methods have extended the vanilla GCN in EA task to incorporate anisotropic attention mechanisms [10], [39]–[43].

However, the relation features are exploited without considering the similarity between entities. Mostly because some of them represent the relation embedding with the same or even twice dimensions [10], [39], [41]–[44] or introduce multi-channel [40] instead of relation embedding for model training, which would be computationally exorbitant.

As a compressed feature of  $e_j$ ,  $r_{e_j}$  merely bring negligible computation incremental. Thus we propose to link the embedding  $\mathbf{h}_{r_k}$  for the  $k$ -th type of relation  $r_k$  to the associated entity scalar weight  $r_{e_j}$  by  $\mathbf{h}_{r_k}^{\rightarrow e_j}$ , when there exists one triples  $\langle e_i, r_k, e_j \rangle$  indicating one edge  $r_k$  from  $e_j$  to  $e_i$ . An orthogonal matrix  $W_r \in \mathbb{R}^{d \times d}$  is applied to  $\mathbf{h}_{r_k}$  to perform projection while preserving its norm for better convergence:

$$\mathbf{h}_{r_k}^{\rightarrow e_j} = r_{e_j} W_r \mathbf{h}_{r_k}, \quad (4)$$

$$L_o = \|W_r^\top W_r - I_{d \times d}\|_2^2, \quad (5)$$

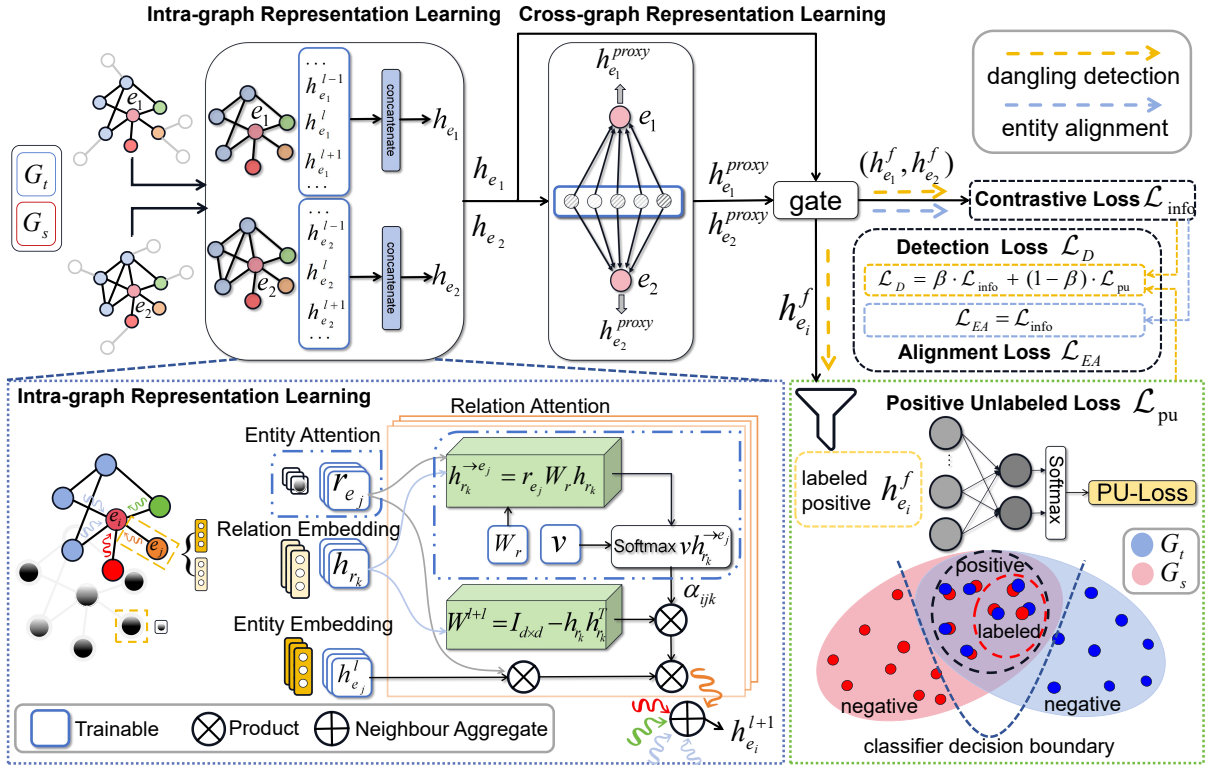


Fig. 2: The illustration of our framework.

where  $L_o$  serves as a regularizer to constrain  $W_r$  to be orthogonal.

To sum up, the attention coefficient is obtained by the following equation:

$$\alpha_{ijk}^l = \frac{\exp(\mathbf{v}^\top \mathbf{h}_{r_k}^{\rightarrow e_j})}{\sum_{e_m \in \mathcal{N}_{e_i}, \langle e_i, r_k, e_m \rangle \in T_s \cup T_t} \exp(\mathbf{v}^\top \mathbf{h}_{r_n}^{\rightarrow e_m})} \quad (6)$$

where  $\mathbf{v}^\top$  is an attention vector.

### B. Intra- & Cross-Graph Representation Learning

Given the entity-relation attention, we can express the embedding of  $e_i$  at the  $l$ -th layer as

$$\mathbf{h}_{e_i}^{l+1} = \sigma \left( \sum_{e_j \in \mathcal{N}_{e_i}, \langle e_i, r_k, e_j \rangle \in T_s \cup T_t} \tanh(r_{e_j}) \alpha_{ijk}^l W^{l+1} \mathbf{h}_{e_j}^l \right),$$

$$W^{l+1} = I_{d \times d} - 2\mathbf{h}_{r_k} \mathbf{h}_{r_k}^\top,$$

where we adopt the  $\tanh(\cdot)$  as the activation function. The entity features  $\mathbf{h}_{e_i}^l$  and relation features  $\mathbf{h}_{r_k}$  are collectively expressed as  $H^e \in \mathbb{R}^{|\mathcal{E}_s \cup \mathcal{E}_t| \times d}$  and  $H^r \in \mathbb{R}^{|\mathcal{R}_s \cup \mathcal{R}_t| \times d}$ . Instead of a standard linear transformation, we apply the Householder transformation  $W^{l+1}$  on  $\mathbf{h}_{e_i}^l$  to restore the relative positions of KGs entities at each layer, so that deeper layers still learn useful features. Overall, the *intra-graph representation* of  $e_i$  is obtained by concatenating embeddings from all layers:

$$\mathbf{h}_{e_i} = [\mathbf{h}_{e_i}^0 \parallel \mathbf{h}_{e_i}^1 \parallel \dots \parallel \mathbf{h}_{e_i}^l]. \quad (7)$$

The aforementioned embedding function applies to each entity on either the source or the target graph. We adopt the *Proxy Matching Attention Layer* proposed by [39] to align the embeddings across two graphs through proxy  $\mathbf{q}_j$  of the same shape with the embedding. For each entity  $e_i$ , on the source or target graph, its *cross-graph representation* can be written as

$$\mathbf{h}_{e_i}^{proxy} = \sum_{q_j \in S_p} \frac{\exp(\text{sim}(\mathbf{h}_{e_i}, \mathbf{q}_j))}{\sum_{q_k \in S_p} \exp(\text{sim}(\mathbf{h}_{e_i}, \mathbf{q}_k))} (\mathbf{h}_{e_i} - \mathbf{q}_j), \quad (8)$$

where  $S_p$  represents the set of proxy vectors, and  $\text{sim}(\cdot)$  denotes the cosine similarity.

Finally, we employ a gating mechanism [45] to integrate both intra-graph representation  $\mathbf{h}_{e_i}$  and cross-graph representation  $\mathbf{h}_{e_i}^{proxy}$  into  $\mathbf{h}_{e_i}^f$ :

$$\theta_{e_i} = \text{sigmoid}(\mathbf{W}_g \mathbf{h}_{e_i}^{proxy} + \mathbf{b}), \quad (9)$$

$$\mathbf{h}_{e_i}^f = [(\theta_{e_i} \cdot \mathbf{h}_{e_i} + (1 - \theta_{e_i}) \cdot \mathbf{h}_{e_i}^{proxy}) \parallel r_{e_i}], \quad (10)$$

where  $\mathbf{W}_g$  and  $\mathbf{b}$  are the gate weight and gate bias, respectively. The learnable weight of  $e_i$  at the final layer is also attached to the embedding.

Note that both the intra- and cross-graph representation learning modules are adopted in the dangling entity detection and the entity alignment stages, yet trained with different losses which we will introduce in the following section.

### C. Contrastive Learning

For entity alignment, we expect a unified feature space where the distance between aligned anchor node pairs to be as close as possible, and the distance between unaligned entity pairs to be as far as possible. Specifically, given a matchable entity  $e_i \in \mathcal{X}_p$ , let there be a paired positive sample entity  $e_+^i \in \mathcal{X}_p$ , such that  $(e_i, e_+^i) \in S$ , and  $N$  sampled entity  $\{e_j^i\}^N$  as negative samples  $(e_i, e_j^i) \notin S$ . To satisfy this intuition, we introduce an alignment loss:

$$H(e_i, e_+^i, e_j^i) = [\text{sim}(e_i, e_j^i) - \text{sim}(e_i, e_+^i) + \gamma]_+, \quad (11)$$

$$\text{sim}(e_i, e_j) = \|\mathbf{h}_{e_i}^f - \mathbf{h}_{e_j}^f\|_2^2, \quad (12)$$

where  $[x]_+$  represents the operation  $\max(0, x)$ . We set  $\text{sim}(\cdot)$  as the  $L_2$ -norm distance between the embeddings to measure the similarity between entities, and a soft margin  $\gamma$  involved to discourage trivial solutions, e.g.,  $\text{sim}(e_i, e_j^i) = \text{sim}(e_i, e_+^i) = 0$ . We set  $\text{sim}(\cdot)$  as the  $L_2$ -norm distance between the embeddings to measure the similarity between entities.

For our proposed dangling entity detection, the vital task is to discriminate the dangling entities from the matchable ones without labeled dangling entities. Hence it is important to separate them in the feature space, which an unsupervised method of spectral clustering could achieve. We design the loss function according to the following **Lemma 1** to achieve its equivalent effect.

**Lemma 1:** *Given one positive sample  $p^+$  for  $q$ , and  $N$  negative samples  $\{p_j^-\}^N$ . Employ the following loss function is equivalent to conducting spectral clustering on similarity graph  $\pi$  in the temperature hyper-parameter  $\lambda$ , whose node-set consists of  $\{q, p^+\} \cup \{p_j^-\}^N$ :*

$$\text{infoNCE}(q, p^+, \{p_j^-\}^N) = -\log \frac{\exp(\lambda \text{sim}(q, p^+))}{\sum_j \exp(\lambda \text{sim}(q, p_j^-))}.$$

The equivalence has been strictly discussed in previous studies [46]–[49]. Regarding our proposed problem, the positive samples are the corresponding pairs whereas the negative samples are those sampled unaligned pairs. We first derive the equivalent form of  $\text{infoNCE}(q, p^+, \{p_j^-\}^N)$  as follows:

$$\log \left[ 1 + \sum_j \exp(\lambda \text{sim}(q, p^+) - \lambda \text{sim}(q, p_j^-)) \right].$$

It is partially replaced using the alignment loss as margin-based fine-tuning:

$$\mathcal{L}(e_i, e_+^i, \{e_j^i\}^N) = \log \left[ 1 + \sum_j \exp(\lambda H(e_i, e_+^i, e_j^i)) \right].$$

Overall, the contrastive learning loss is:

$$\mathcal{L}_{\text{info}} = \sum_{e_i \in \mathcal{X}_p} \mathcal{L}(e_i, e_+^i, \{e_j^i\}^N). \quad (13)$$

Minimizing the contrastive loss of Eq. (13) maps matchable and dangling entities into different feature spaces for improved detection accuracy while facilitating entity alignment. In practice, we adopt the loss normalization trick [28] on  $H(\cdot)$  to speed up training.

### D. Positive-Unlabeled Dangling Detection

The previous dangling detection approach usually requires the label information of a subset of dangling and matchable entities and sees the detection problem as a supervised classification one [4], [15]. However, it is common in the real world that the labels for the dangling entities are missing, as those labels are much harder to acquire than those of matchable ones. For example, one can quickly query a source entity locally in (a part of) the target graph to locate an aligned pair, but to claim the source entity has no matches would have to traverse the entire target graph, which is particularly infeasible if the target graph is orders of magnitude larger than the source graph.

To better fit such a scenario, we propose to replace the conventional positive-negative learning with positive-unlabeled (PU) learning to relieve the dependence on the labeled dangling entities. The positive samples refer to those matchable entities whereas the negative ones are dangling entities. The distinction from the representative work of previous work [18] is that: the following derivation restricts nothing on the distribution of unlabeled samples  $p_u(x)$ , rendering it applicable to general binary classification PU learning scenarios.

**Theorem 1:** *Suppose that  $g \in \mathcal{G} : \mathbb{R}^d \rightarrow \mathbb{R}$  be an binary classifier, and  $\ell : \mathbb{R} \times \{\pm 1\} \rightarrow \mathbb{R}$  be the loss function, such that the value  $\ell(t, y)$  means the loss incurred by predicting an output  $t$  when the ground truth is  $y$ .  $R(g)$  can be approximated indirectly by:*

$$\widehat{R}_{\text{pu}}(g) = \pi_p \widehat{R}_p^+(g) + \frac{\pi_n}{\pi_n^u} \cdot \left[ \widehat{R}_u^-(g) - \pi_p^u \widehat{R}_p^-(g) \right], \quad (14)$$

which is the **unbiased risk estimator** of  $R(g)$ , where  $\pi_p^u = p_u(y = +1)$  and  $\pi_n^u = p_u(y = -1)$  are the **class-prior probability**.  $R_p^+(g) = \mathbb{E}_{X \sim p_p(x)}[\ell(g(X), +1)]$  and  $R_n^-(g) = \mathbb{E}_{X \sim p_n(x)}[\ell(g(X), -1)]$  are the **risk of positive and negative samples respectively**.

**Positive Unlabeled Loss Function.** Since it is evident that  $\frac{\pi_n}{\pi_n^u} < 1$ , we apply a hyper-parameter  $\alpha > 1$  to scale  $\pi_p \widehat{R}_p^+(g)$  equivalently. The PU learning loss function guaranteeing  $\pi_n R_n^-(g) \geq 0$  is formulated as:

$$\mathcal{L}_{\text{pu}} = \alpha \pi_p \widehat{R}_p^+(g) + \max\{0, \widehat{R}_u^-(g) - \pi_p^u \widehat{R}_p^-(g)\},$$

We specify the corresponding risk function using cross-entropy loss function  $CE(\cdot)$ , 0 and 1 are binary labels for matchable

and dangling entities respectively:

$$\begin{aligned}\widehat{R}_p^+(g) &= \sum_{x_p \in \mathcal{X}_p} CE(z[x_p], 0), \\ \widehat{R}_u^-(g) &= \sum_{x_u \in \mathcal{X}_u} CE(z[x_u], 1), \\ \widehat{R}_p^-(g) &= \sum_{x_p \in \mathcal{X}_p} CE(z[x_p], 1),\end{aligned}$$

where the output label  $z[x] = \text{softmax}(\text{MLP}(h_x^f))$  is based on GNN final output embedding  $h_x^f$ . Hence each term in the final loss can be calculated or estimated without the negative labels.

### E. Risk Bound and Algorithm

We derive the risk bound of our PU learning  $\widehat{R}_{\text{pu}}(g)$  of Eq. (14), and show it is a tighter uniform deviation bound compared with that of *Non-negative Risk Estimator* [18].

**Theorem 2:** Let  $\text{Var}(R)$  denotes the uniform deviation bound of risk estimator  $R$ , and *Non-negative Risk Estimator* be  $\widehat{R}'_{\text{pu}}(g)$ , then:

$$\text{Var}(\widehat{R}_{\text{pu}}(g)) < \text{Var}(\widehat{R}'_{\text{pu}}(g)). \quad (15)$$

**The overall algorithm.** Our framework comprises two GNN-based encoders sharing the same structure with separate loss functions, corresponding to dangling entity detection and entity alignment. The GNN-based encoder takes as input triples of two KGs and pre-aligned anchor node pairs as training data. Our method is valid across different datasets. With the help of pre-aligned anchor node pairs, arbitrary KGs that can be expressed as triples could be handled. For dangling entity detection, the loss  $\mathcal{L}_D$  is a combination of  $\mathcal{L}_{\text{info}}$  and  $\mathcal{L}_{\text{pu}}$  that

$$\mathcal{L}_D = \beta \cdot \mathcal{L}_{\text{info}} + (1 - \beta) \cdot \mathcal{L}_{\text{pu}}, \beta \in (0, 1). \quad (16)$$

The loss for entity alignment is  $\mathcal{L}_{EA} = \mathcal{L}_{\text{info}}$ .

During the testing phase, the DED results are provided in the inference phase of EA. Removing the dangling entities predicted, we perform entity alignment on the rest entities. To address the hubness problem in high-dimensional space, CSLS [50] is adopted as the distance metric to choose the pairs with the minimal distance as aligned.

## V. EXPERIMENTS

We evaluate our method on real-world datasets: DBP15K, DBP2.0, GA16K, and MedED. All attributes are removed from the datasets so that only graph structure information can be used. The experimental setup is introduced in Sec. V-A whereas the results are displayed from Sec. V-B to Sec. V-D. We aim to answer the following research questions with our experiments:

**RQ1:** How do current network alignment methods perform in unlabeled dangling cases?

**RQ2:** How does our method compare with dangling-entities-unaware baselines?

Datasets		# Entities	# Rel.	# Triples	# Dang	# Align
DBP2.0 <sub>ZH-EN</sub>	Chinese	84,996	3,706	286,067	51,813	33,183
	English	118,996	3,402	586,868	85,813	
DBP2.0 <sub>JA-EN</sub>	Japanese	100,860	3,243	347,204	61,090	39,770
	English	139,304	3,396	668,341	99,534	
DBP2.0 <sub>FR-EN</sub>	French	221,327	2,841	802,678	97,375	123,952
	English	278,411	4,598	1,287,231	154,459	
DBP15K <sub>ZH-EN</sub>	Chinese	19,388	1,701	70,414	4,388	15,000
	English	19,572	1,323	95,142	4,572	
DBP15K <sub>JA-EN</sub>	Japanese	19,814	1,299	77,214	4,814	15,000
	English	19,780	1,153	93,484	4,780	
DBP15K <sub>FR-EN</sub>	French	19,661	903	105,998	4,661	15,000
	English	19,993	1,208	115,722	4,993	
MedED <sub>ES-EN</sub>	Spanish	19,639	537	610,489	8,339	11,300
	English	18,855	614	855,467	7,555	
MedED <sub>FR-EN</sub>	French	19,109	431	449,277	12,672	6,437
	English	18,855	614	855,467	12,418	
GA16K	None	6,208	8	68,534	0	6,208
	None	16,363	12	151,662	10,155	

TABLE II: Statistics of DBP2.0, DBP15K, MedED and GA16K.

**RQ3:** How does our dangling entities detection module work?

**RQ4:** How does our method compare with dangling-entities-aware baselines?

**RQ5:** How does each module contribute to the entirety?

**RQ6:** How does our method perform with different proportions of labeled entities and feature dimensions?

**RQ7:** What is the actual efficiency of our approach?

### A. Setup

**Datasets.** The training/test sets for each dataset are generated using a fixed random seed. For entity alignment, 30% of matchable entity pairs constitute the training set, while the remaining form the test set. For dangling entity detection, we did not utilize any labeled dangling entity data, in contrast to prior work which labels 30% of the dangling entities and matchable pairs respectively for training [15]. Hence our method imposes minimal restrictions on annotated data. All datasets are briefly introduced in the following and some statistics are provided in Tab. II.

DBP15K [51]: DBP15K consists of three cross-lingual subsets constructed from DBpedia: English-French(DBP<sub>FR-EN</sub>), English-Chinese (DBP<sub>ZH-EN</sub>), English-Japanese(DBP<sub>JA-EN</sub>). Each subset contains 15,000 pre-aligned entity pairs. This dataset includes a small proportion of dangling entity samples which is yet mostly ignored in previous entity alignment tasks.

DBP2.0 [15]: DBP2.0 is an entity alignment dataset with a considerable proportion of dangling entities, constructed from the multilingual Infobox Data of DBpedia [52]. The dataset contains three pairs of crosslingual KGs, ZH-EN (Chinese to English), JA-EN (Japanese to English), and FR-EN (French to English). Since there are dangling nodes in both the source and target graphs, we separately test source-to-target and target-to-source alignment, consistent with the established approach. A representative feature of the dataset is that the matchable and dangling entities exhibit similar degree distributions which

are hard to distinguish, displaying a real-world challenge in aligning knowledge graphs.

**MedED [17]:** MedED is constructed from the Unified Medical Language System (UMLS) [53]. Concepts within UMLS are associated with multiple terms in various languages. MedED is not fully released and we follow the methods of [17] to extract the KGs in three languages — English, French, and Spanish, and compose FR-EN (French to English) and ES-EN (Spanish to English) paired datasets. We selected 20,000 entities from the UMLS with the most triples in each specified language for both dangling entity detection and entity alignment.

**GA16K:** This dataset constructed by us exclusively contains dangling nodes in the target graph, facilitating a comparison between our work and baselines that neglect dangling entities. GA16K is extracted from GAKG [54], a multimodal Geoscience Academic Knowledge Graph. We first order each type of entity in GAKG according to their degrees and select the entities with a large degree into the entity set. A total of 16,363(16K) separate entities and their relations were extracted to compose the target graph. Then we extract 6,208 entities from the target graph to comprise the source graph. Hence there are 6,208 ground-truth matchable pairs between the source and the target. The remaining 10,155 entities in the target graph are regarded as dangling entities.

**Baselines.** Since our work does not take advantage of any side information, we emphasize its comparison with the previous methods purely depending on graph structures. These works majorly incorporate two types:

*Dangling-Entities-Unaware.* We include advanced entity alignment methods in recent years: GCN-Align [7], RSNs [55], MuGNN [40], KECG [41]. Methods with bootstrapping to generate semi-supervised structure data are also adopted: BootEA [11], TransEdge [56], MRAEA [10], AliNet [8], and Dual-AMN [39].

*Dangling-Entities-Aware.* To the best of our knowledge, the method of [15] is the most fairly comparable baseline which is based on MTransE [16] and AliNet [8]. Because MHP [35] over-emphasized the use of labeled dangling data, while SoTead [36] and UED [4] utilize additional side-information. We exclude them from baselines for our methods. [15] introduces three techniques to address the dangling entity issue: nearest neighbor (NN) classification, marginal ranking (MR), and background ranking (BR). Since BR outperforms other techniques, we solely combine MTransE with BR as our baseline on MedED.

## B. Experiments Unaware of Dangling Entities

We show the experiments on baselines without considering dangling entities in this section. We first illustrate the performance decay of existing approaches when dangling entities are taken into account, and then compare entity alignment performance against those baselines in the consolidated setting.

**Performance Decay Caused by Dangling Entities (RQ1).** We reproduce the baselines unaware of dangling entities on DBP15K in the relaxed setting. On the same dataset, we

rerun their methods but in a consolidated setting that takes the dangling entities into account. Even though DBP15K only comprises a small percentage of dangling entities, the drop in the consolidated setting is significant, as shown in Tab. III.

The reason behind such a performance drop is mainly because most previous works remove dangling entities from the ground truth in measuring their alignment performance. In particular, Dual-AMN takes advantage of the bootstrapping module by incorporating labeled pairs in training. In the relaxed setting, such labeled pairs are ground-truth aligned pairs, but in the consolidated setting, the dangling entities could bring in erroneous alignment which contaminates the alignment of other pairs.

**Dangling-Entities-Unaware Baselines Comparison (RQ2).** The direct comparison between our method and the dangling-entities-unaware baselines is unavailable due to different metrics being used in relaxed and consolidated settings. To establish a fair and common ground, we adopt the GA16K dataset for comparison since the dataset exclusively contains dangling nodes in the target graph. Thus the ranking list  $S$  in Hits@K only contains (matchable) entities in the source graph, which is in line with the metric of the baselines. Moreover, we do not remove any detected dangling entities in training, further aligning the baselines.

In Tab. IV, Dual-AMN demonstrates a competitive performance but is inferior to ours at Hits@1. The reason that Dual-AMN enjoys such high performance is that it splits the triples  $\langle h, r, t \rangle$  into two triples  $\langle h, r', t \rangle$  and  $\langle t, -r', h \rangle$ , which doubles the number of edges in the graph. Specifically for GA16K, the original relation information is scarce with no more than 20 types, and thus the trick significantly boosts the performance of representation learning. We also adopt their ‘edge-doubling’ trick in our method if memory is permitted. MRAEA shares a similar performance to Dual-AMN since the latter is built on the former. TransEdge performs poorly since the method adopts semi-supervised bootstrapping to iteratively add newly identified aligned pairs to the training set. The presence of dangling entities could lead to mismatch and the error may propagate to other entities. Meanwhile, TransEdge is a relation-centric approach that suffers from insufficient relation information on GA16K. The poor performance of RSNs can be explained by the impact of uneven distribution of GA16K. Other baselines exhibit up-to-par performance but our method delivers consistently superior or state-of-the-art accuracy across all Hits@Ks.

## C. Experiments Aware of Dangling Entities

In this section, we provide experimental results on dangling detection and entity alignment, compared with baselines aware of dangling entities.

**Dangling Entities Detection Performance (RQ4).** We test the dangling entities detection performance of our method in comparison with baselines that are aware of dangling entities. The results on DBP2.0 in the consolidated setting are reported in Tab. V. Note that the comparison is actually not fair as our method uses less information than the baselines. Ours



Method	DBP15K <sub>ZH-EN</sub>			DBP15K <sub>JA-EN</sub>			DBP15K <sub>FR-EN</sub>		
	H@1	H@10	H@50	H@1	H@10	H@50	H@1	H@10	H@50
BootEA	31.30↓ 20.96	59.70↓ 16.18	71.51↓ 12.91	33.77↓ 15.27	62.66↓ 11.64	73.09↓ 10.29	23.11↓ 26.72	58.39↓ 18.77	71.54↓ 14.00
TransEdge	49.91↓ 15.21	76.62↓ 9.79	83.44↓ 7.16	54.07↓ 13.42	78.01↓ 8.25	84.00↓ 6.21	48.23↓ 17.34	79.32↓ 9.70	86.69↓ 6.24
MRAEA	59.45↓ 5.62	83.04↓ 2.53	88.68↓ 1.56	61.60↓ 4.45	83.48↓ 2.21	88.65↓ 1.50	61.55↓ 6.62	85.85↓ 2.61	90.79↓ 1.69
GCN-Align	31.99↓ 10.70	62.21↓ 6.45	71.93↓ 4.31	32.08↓ 10.08	61.04↓ 5.86	70.34↓ 3.52	30.71↓ 10.50	61.64↓ 7.07	72.45↓ 5.55
RSNs	43.00↓ 8.50	62.90↓ 8.00	69.70↓ 7.00	20.60↓ 31.60	44.60↓ 26.60	53.20↓ 23.60	36.30↓ 15.30	63.30↓ 10.10	71.70↓ 7.80
MuGNN	34.66↓ 14.75	68.48↓ 9.32	80.53↓ 5.69	32.93↓ 14.68	66.68↓ 8.82	78.63↓ 5.67	34.93↓ 14.02	68.88↓ 9.69	81.67↓ 5.32
KECG	35.92↓ 12.87	65.70↓ 10.35	76.44↓ 8.06	32.31↓ 15.48	63.19↓ 11.96	74.42↓ 9.29	32.84↓ 15.47	64.78↓ 11.98	76.70↓ 8.35
AliNet	53.84↓ 0.66	73.73↓ 3.16	80.30↓ 1.59	52.69↓ 1.30	74.01↓ 2.60	80.91↓ 1.90	54.01↓ 0.58	76.19↓ 2.74	83.25↓ 1.40
Dual-AMN	60.72↓ 12.20	83.93↓ 5.22	89.45↓ 3.54	62.29↓ 10.62	83.38↓ 5.35	88.80↓ 3.21	65.33↓ 10.48	87.76↓ 4.17	92.47↓ 2.24

TABLE III: Network alignment performance on DBP15K in the consolidated setting. The blue numbers suggest the drop from the relaxed setting (as with their original implementation).

Method	GA16K		
	H@1	H@10	H@50
BootEA	13.95	37.25	49.08
TransEdge	0.03	0.12	0.14
MRAEA	63.97	76.64	81.06
GCN-Align	29.48	45.64	57.15
RSNs	9.40	42.70	46.70
MuGNN	62.17	76.25	80.87
KECG	44.18	57.73	63.41
AliNet	48.53	67.72	74.50
Dual-AMN	<u>64.49</u>	<b>80.55</b>	<b>84.67</b>
Ours	<b>67.59</b>	<u>80.33</u>	<u>84.35</u>

TABLE IV: Performance comparison with dangling-entities-unaware baselines on GA16K. The best and second-best performance is marked in bold and underscored, respectively.

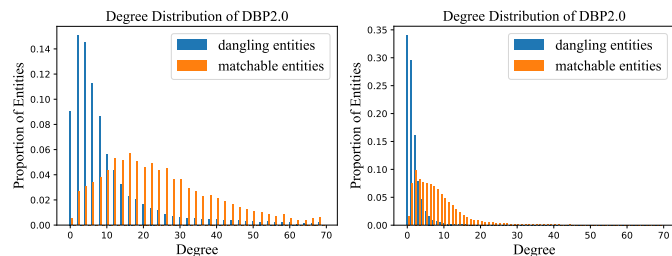


Fig. 3: Degree distribution for the dangling and matchable entities in DBP2.0 and MedED (FR-EN).

do not use the 30% of the labeled dangling entities as the baselines. Nevertheless, our approach maintains state-of-the-art performance across all six datasets, excelling in almost every metric except for a slightly inferior precision. Then we pick the optimal baseline in Tab. V, i.e., MtransE(BR), to perform dangling entities detection on MedED, with results reported in Tab. VI. Our performance still remains close to the baseline performance. As we look into the degree distribution of the two datasets in Fig. 3, it is clear that the distributions are harder to distinguish on MedED than on DBP2.0, which accounts for the inferior detection accuracy on MedED.

#### How does our dangling entities detection module work?

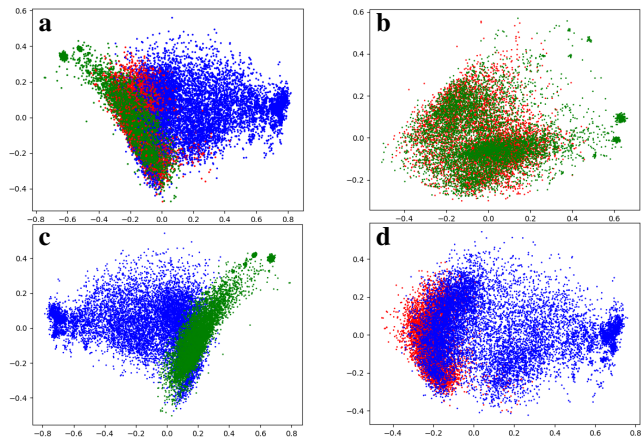


Fig. 4: Visualization of entity representations learned by our method on GA16K dataset. Different colors denote different classes of nodes. Red for matchable entity in the source KG, green for matchable entity in the target KG and blue for dangling entities.

**(RQ3).** To understand why our method works and why the precision slightly suffers, we visualized all entity embeddings of GA16K in Fig. 4. For a clearer view, we denote the matchable entities in the source in red, the matchable entities in the target in green, and the dangling nodes in blue. We depict four subfigures with each showing a different combination of the three types of nodes. The distribution of all three types of nodes in Fig. 4(a) suggests that our method maps all nodes into a unified embedding space where the matchable ones in source and target significantly overlap (shown in Fig. 4(b)). It essentially displays the power of our method in aligning matchable pairs. Fig. 4(c)(d) depicts that a part of the dangling entities is intertwined with the matchable ones, suggesting that this part resides at the decision boundary and easily leads to false positives. It could in part explain the lesser precision of our method.

#### Dangling-Entities-Aware Baselines Comparison (RQ4).

In Tab. VIII, we report the entity alignment performance of our method in the more realistic consolidated setting on DBP2.0. Our method undergoes two stages: the first is dangling entities detection and the second is entity alignment with the dangling entities removed.

Methods	ZH-EN			EN-ZH			JA-EN			EN-JA			FR-EN			EN-FR			
	Prec.	Rec.	F1	Prec.	Rec.	F1	Prec.	Rec.	F1	Prec.	Rec.	F1	Prec.	Rec.	F1	Prec.	Rec.	F1	
AliNet	NNC	.676	.419	.517	.738	.558	.634	.597	.482	.534	.761	.120	.207	.466	.365	.409	.545	.162	.250
	MR	.752	.538	.627	.828	.505	.627	.779	.580	.665	.854	.543	.664	.552	.570	.561	.686	.549	.609
	BR	.762	.556	.643	.829	.515	.635	.783	.591	.673	.846	.546	.663	.547	.556	.552	.674	.556	.609
MTransE	NNC	.604	.485	.538	.719	.511	.598	.622	.491	.549	.686	.506	.583	.459	.447	.453	.557	.543	.550
	MR	.781	.702	.740	.866	.675	.759	.799	.708	.751	.864	.653	.744	.482	.575	.524	.639	.613	.625
	BR	<b>.811</b>	<b>.728</b>	<b>.767</b>	<b>.892</b>	<b>.700</b>	<b>.785</b>	<b>.816</b>	<b>.733</b>	<b>.772</b>	<b>.888</b>	<b>.731</b>	<b>.801</b>	.539	.686	.604	.692	.735	.713
Ours	.763	<b>.925</b>	<b>.836</b>	.844	<b>.909</b>	<b>.875</b>	<b>.807</b>	<b>.836</b>	<b>.821</b>	<b>.880</b>	<b>.809</b>	<b>.843</b>	<b>.615</b>	<b>.772</b>	<b>.685</b>	<b>.732</b>	<b>.749</b>	<b>.740</b>	

TABLE V: Dangling detection results on DBP2.0 in the consolidated setting.

Methods	ES-EN			FR-EN		
	Prec.	Rec.	F1	Prec.	Rec.	F1
MtransE(BR)	<b>.684</b>	<b>.838</b>	<b>.753</b>	<b>.894</b>	.751	.817
Ours	.617	.789	.692	.753	<b>.973</b>	<b>.849</b>

TABLE VI: Dangling detection results on MedED in the consolidated setting.

Overall, our method enjoys superior recall and F1 score with adequate precision. Upon closer examination of F1 and recall metrics, the substantial gap between our performance and the second-best one underscores the advanced capabilities of our approach. Given that no labeled dangling entities are used in training, our method shows outstanding strength in capturing the distribution of dangling entities. To match as many pairs as possible, it is a strategy to classify more entities as matchable in the detection stage. Thus it is reasonable to trade precision (with a higher false positive) for an improved recall to boost the alignment performance.

The alignment performance on MedED is reported in Tab. VII. Affected by the inferior detection performance (Tab. VI), the precision and F1 score of the alignment task are lower than those of MtransE(BR), but our method surpasses the baseline in terms of Hits@1 (in the consolidated setting) and recall, showing adequate performance considering no dangling labels are used in our training procedure.

Methods	ES-EN				FR-EN			
	Hits@1	Prec.	Rec.	F1	Hits@1	Prec.	Rec.	F1
MtransE(BR)	.755	<b>.737</b>	.627	<b>.678</b>	.684	<b>.504</b>	.658	<b>.571</b>
Ours	<b>.919</b>	.604	<b>.734</b>	.663	<b>.897</b>	.398	<b>.784</b>	.528

TABLE VII: Entity alignment results on MedED in the consolidated setting.

#### D. Ablation Studies

In this section, we conduct ablation studies to understand the role of each module in our design, and how hyperparameters impact the overall performance.

**Effect of Entity and Relation Attention (RQ5).** We test the impact of the entity attention  $r_{e_i}$  and the relation attention  $\mathbf{h}_{r_k}^{\rightarrow e_j}$  to the outcome by removing them from the

system, respectively. We denote the counterpart removing  $r_{e_i}$  as  $w/o r_{e_i}$ , and the counterpart replacing  $\mathbf{h}_{r_k}^{\rightarrow e_j}$  with the original  $\mathbf{h}_{r_k}$  as  $w/o \mathbf{h}_{r_k}^{\rightarrow e_j}$ .

Fig. 5 gives the ablation study results on DBP2.0, where ‘Ours’ represents an all-inclusive version of our design. We observe that the relation attention has a more substantial impact than entity attention to the alignment performance. This shows the important role of relation attention in the alignment task with dangling entities.

As to why the entity attention has a minor impact on the alignment, we consider it may be attributed to the lower degrees of dangling entities on DBP2.0, as depicted in Fig. 3. As the figure shows, the degrees of dangling entities are generally lower than that of matchable ones, indicating that the dangling nodes are more isolated in the graph and thus have less impact on matchable nodes in the neighborhood aggregation of GCN. Meanwhile, relation embeddings learn by relation types and thus are less affected by the connectivity of the nodes. A similar conclusion can be drawn on Tab. IX for MedED where dangling entities are generally of lower degrees than the matchable ones as shown in Fig. 3.

**Varying Anchor Nodes (RQ6).** Pre-aligned entities may be far scarce in real-world scenarios. We investigate the sensitivity of our method to the variation in the proportion of pre-aligned anchor nodes. As the proportion increases, the alignment performance enhances as provided in Fig. 6. Notably, even with an anchor ratio as low as 5%, our alignment accuracy still well exceeds 30% on most source-target datasets except for FR-EN and EN-FR.

We attribute the underperformance to the large-scale graph structure of FR-EN and EN-FR. The two datasets contain twice as many entities and triples as ZH-EN and FR-EN, which introduces intricate dependencies among entities and thus greater challenges in alignment. Moreover, a larger graph may require a higher dimension of representations to learn, but the embedding dimension is restricted to merely 96 due to the out-of-memory problem.

**Embedding Dimension Selection (RQ6).** Although a higher embedding dimension may encode richer information, an overly high dimension leads to performance decline. We select the GNN dimension according to the principle of [36]. Let the dimension of embedding be  $d$  and the number of entities is  $N$ . According to the feature entropy in [36], it holds

Methods	ZH-EN			EN-ZH			JA-EN			EN-JA			FR-EN			EN-FR			
	Prec.	Rec.	F1	Prec.	Rec.	F1	Prec.	Rec.	F1	Prec.	Rec.	F1	Prec.	Rec.	F1	Prec.	Rec.	F1	
AliNet	NNC	.121	.193	.149	.085	.138	.105	.113	.146	.127	.067	.208	.101	.126	.148	.136	.086	.161	.112
	MR	.207	.299	.245	.159	.320	.213	.231	.321	.269	.178	.340	.234	.195	.190	.193	.160	.200	.178
	BR	.203	.286	.238	.155	.308	.207	.223	.306	.258	.170	.321	.222	.183	.181	.182	.164	.200	.180
MTransE	NNC	.164	.215	.186	.118	.207	.150	.180	.238	.205	.101	.167	.125	.185	.189	.187	.135	.140	.138
	MR	<u>.302</u>	.349	.324	<u>.231</u>	.362	.282	.313	.367	<u>.338</u>	.227	.366	.280	<u>.260</u>	<u>.220</u>	<u>.238</u>	<u>.213</u>	<u>.224</u>	.218
	BR	<b>.312</b>	<u>.362</u>	<u>.335</u>	<b>.241</b>	<u>.376</u>	<u>.294</u>	<u>.314</u>	.363	<u>.336</u>	<b>.251</b>	<u>.358</u>	<u>.295</u>	<b>.265</b>	<u>.208</u>	<u>.233</u>	<b>.231</b>	.213	<u>.222</u>
Ours	.279	<b>.447</b>	<b>.344</b>	.219	<b>.489</b>	<b>.303</b>	<b>.324</b>	<b>.409</b>	<b>.362</b>	<u>.234</u>	<b>.460</b>	<b>.310</b>	.234	<b>.320</b>	<b>.271</b>	.192	<b>.363</b>	<b>.251</b>	

TABLE VIII: Entity alignment results on DBP2.0 in the consolidated setting.

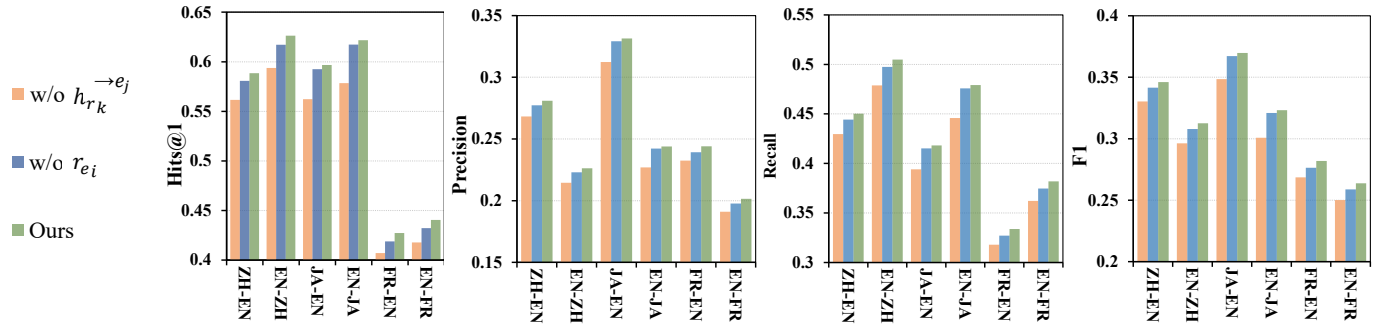


Fig. 5: The entity alignment performance with or without entity and relation attention in the consolidated setting on DBP2.0.

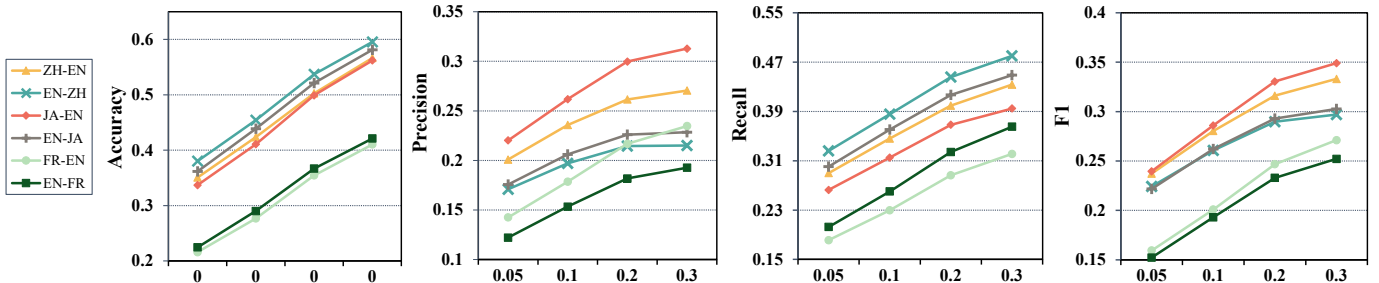


Fig. 6: The entity alignment performance on varying pre-aligned anchor nodes ratios on DBP2.0.

Methods	ES-EN				FR-EN			
	Hits@1	Prec	Rec	F1	Hits@1	Prec	Rec	F1
w/o $h_{r_k} \rightarrow e_j$	.881	.579	.704	.635	.889	.443	.323	.373
w/o $r_{e_l}$	.911	.599	.728	.657	.902	.449	.327	.379
Ours	.917	.603	.733	.662	.930	.463	.338	.391

TABLE IX: The entity alignment performance with or without entity and relation attention on MedED.

that  $d > 8.33 \log N$  by the Johnson-Lindenstrauss lemma [57] that the vector dimension is at  $\mathcal{O}(\log N)$  order. In most of our settings,  $N$  is approximately  $10^5$ , and thus  $d$  is set to 128.

As shown in Tab. X, due to the varying number of entities in datasets, the embedding dimension at the optimal performance varies. For example, the top performance is achieved on ZH-EN and EN-ZH when the embedding dimension is 96 but is obtained on JA-EN, EN-JA, FR-EN, and EN-FR with an embedding dimension of 128. As a compromise, we remove the ‘edge-doubling’ trick of Dual-AMN (Sec. V-B) to enable

FR-EN and EN-FR to run with an embedding dimension of 128 with limited memory. A higher alignment performance can be achieved if no compromise is made. As we observe, the optimal performance is typically achieved at the theoretically chosen  $d$ . This also indicates our approach has a memory cost at the order of  $\mathcal{O}(\log N)$ .

### E. Efficiency

**(RQ7):** The previous works concerning the dangling problem have not analyzed its efficiency in their experiments. Thus we only report the efficiency of our methods without baseline comparison. We evaluate the efficiency of our work on Tab. XI including alignment search time as ‘Inference Time’, GNN encoder average training time as ‘Average Training Time’, and GPU memory cost on three different datasets of DBP2.0. Data obtained from these three datasets with the top three node numbers is a robust indicator of the efficiency of our method.

We gathered the mean value of 5 inference time costs for each dataset with the corresponding CPU and GPU memory

Dimension	ZH-EN			EN-ZH			JA-EN			EN-JA			FR-EN			EN-FR			
	Prec.	Rec.	F1	Prec.	Rec.	F1	Prec.	Rec.	F1	Prec.	Rec.	F1	Prec.	Rec.	F1	Prec.	Rec.	F1	
Ours	64	.278	.446	.342	.224	.501	.310	.325	.410	.362	.239	.470	.317	.164	.224	.189	.135	.257	.178
	96	<b>.281</b>	<b>.451</b>	<b>.346</b>	<b>.226</b>	<b>.505</b>	<b>.312</b>	.329	.415	.367	.241	.474	.320	.172	.235	.199	.143	.271	.187
	128	.280	.448	.344	.225	.502	.311	<b>.330</b>	<b>.416</b>	<b>.368</b>	<b>.243</b>	<b>.477</b>	<b>.322</b>	<b>.177</b>	<b>.242</b>	<b>.204</b>	<b>.151</b>	<b>.287</b>	<b>.198</b>

TABLE X: The entity alignment performance over different embedding dimensions on DBP2.0.

Datasets	Triples	Inference Time	Average Training Time (from 1 to 45 training epochs)						CPU Memory	GPU Memory
			1-20	21-25	26-30	31-35	36-40	41-45		
DBP2.0 <sub>ZH-EN</sub>	872,935	48.78s	11.21s/it	21.16s/it	25.67s/it	28.17s/it	29.21s/it	30.14s/it	10.8GB	32.5GB
DBP2.0 <sub>JA-EN</sub>	1,015,545	120.76s	28.14s/it	53.99s/it	63.43s/it	68.27s/it	70.61s/it	72.80s/it	11.9GB	32.6GB
DBP2.0 <sub>FR-EN</sub>	2,089,909	382.48s	90.18s/it	158.18s/it	190.65s/it	-	-	-	27.7GB	60.2GB

TABLE XI: Efficiency performance of our work on DBP2.0. The measurement of average training time is ‘s/it’, which indicates seconds per iteration. One iteration here represents one training epoch. ‘-’ indicates the absence of data due to training termination.

consumption. Meanwhile, the average training time for each period from early to late is calculated. We enumerate the average training time of epochs 1-20, 21-25, 26-30, 31-35, 36-40 and 41-45.

Cause GPU is employed for not only model training but also inference, as shown on Tab XI, the inference speed is still very impressive. Specifically, we split the large similarity matrix into multiple independent row blocks to perform the nearest searches within each block, which are well suited for GPU parallel processing.

It’s noteworthy that the average training time correspondingly increases as training progresses from early to late stages. More quasi-supervised information incorporated by us accounts for that. To be specific, as the training deepens, we repeatedly conduct preliminary alignment tests while we gather more and more entity pairs mutually closest under a given metric. The entity pairs serve as the pre-aligned anchor nodes, i.e., the quasi-supervisory information mentioned above.

Besides, we list the CPU and GPU memory consumption required for our work. Memory consumption is influenced by various factors such as complex allocation algorithms, model parameter scales, and hyperparameters. In this problem, we put more attention on triples which characterize one KG, revealing an approximate proportionality between the number of triples and memory consumption.

### F. Discussion

As we found, the alignment problem with dangling cases has a deeper issue concerning the classification of imbalanced datasets. It originated from the observation that the alignment performance from the source to the target is different from the other direction. The work of [15] has observed that on DBP2.0, choosing the alignment direction from a less populated KG (e.g., ZH, JA, FR) to a more populated KG (e.g., EN) enjoys a higher alignment accuracy but the other way around would lead to a noticeable performance drop. Meanwhile, the dangling entity detection on EN-XX has a higher F1 score than XX-EN, as shown in Tab. XII.

Datasets	Dangling Detection						Entity Alignment		
	Our Work			Trivial			Our Work		
	Prec.	Rec.	F1	Prec.	Rec.	F1	Prec.	Rec.	F1
ZH-EN	.763	<b>.925</b>	.836	.583	<b>1</b>	.736	<b>.279</b>	.447	<b>.344</b>
EN-ZH	<b>.844</b>	.909	<b>.875</b>	<b>.609</b>	<b>1</b>	<b>.756</b>	.219	<b>.489</b>	.303
JA-EN	.807	<b>.836</b>	.821	.580	<b>1</b>	.734	<b>.324</b>	<b>.409</b>	<b>.362</b>
EN-JA	<b>.880</b>	.809	<b>.843</b>	<b>.605</b>	<b>1</b>	<b>.753</b>	.234	.320	.271
FR-EN	.615	<b>.772</b>	.685	.439	<b>1</b>	.610	<b>.234</b>	.320	<b>.271</b>
EN-FR	<b>.732</b>	.749	<b>.740</b>	<b>.554</b>	<b>1</b>	<b>.715</b>	.192	<b>.363</b>	.251

TABLE XII: Dangling entities detection by a our classifier v.s. a trivial one on DBP2.0.

By analysis, we think it may be attributed to an improper indication of the dangling entity detection power on imbalanced datasets. This error in removing the predicted dangling entity would accumulate hurting the alignment task. To verify the point, we introduce a trivial classifier that makes a simple choice to classify all entities as dangling (positive) ones, and the detection results are reported in Tab. XII. As all unlabeled entities are trivially classified as dangling ones, the detection metrics of the trivial classifier are all falsely high. The more populated source KG usually has more dangling entities (positives) and thus yields a higher precision in detection. Meanwhile, since the detection classifier actually is not working, more dangling entities participate in the alignment phase, resulting in poor alignment performance. This has explained why EN-XX has a higher dangling detection performance but a lower alignment accuracy compared to the other direction.

The root of this issue is that matchable and dangling entities comprise imbalanced categories in the classification task, but the corresponding metric is inappropriate. Hence boosting the detection performance does not necessarily improve the alignment performance. We believe more practical indicators of imbalanced datasets should be introduced to the alignment problem.

## VI. CONCLUSION

We found that conventional EA methods suffer from great performance decline if dangling entities are considered as in most real-world scenarios. Our goal is to address the EA problem in the presence of dangling entities which are all unlabeled. We propose a novel GNN-based framework jointly detecting dangling entities and pairing matchable ones. The core idea is to selectively choose useful neighborhood information for aggregation by a new entity-relation attention mechanism and to adopt a positive-unlabeled learning loss for unbiased estimation of dangling entities. Experimental results on multiple representative datasets demonstrate the effectiveness of our proposed approach. This work also has important implications for real-world applications, such as EA across graphs of different scales, KG plagiarism detection, etc.

## REFERENCES

- [1] A. El-Roby and A. Aboulmaga, "Alex: Automatic link exploration in linked data," in *Proceedings of the 2015 ACM SIGMOD International Conference on Management of Data (SIGMOD)*, 2015, pp. 1839–1853.
- [2] R. Isele and C. Bizer, "Learning expressive linkage rules using genetic programming," *Proceedings of the 38th international conference on very large data bases (VLDB)*, vol. 5, no. 11, pp. 1638–1649, 2012.
- [3] F. M. Suchanek, S. Abiteboul, and P. Senellart, "Paris: Probabilistic alignment of relations, instances, and schema," *Proceedings of the 37th international conference on very large data bases (VLDB)*, vol. 5, no. 3, pp. 157–168, 2011.
- [4] S. Luo and S. Yu, "An accurate unsupervised method for joint entity alignment and dangling entity detection," in *Findings of the Association for Computational Linguistics (ACL)*, 2022, pp. 2330–2339.
- [5] K. Xu, L. Wang, M. Yu, Y. Feng, Y. Song, Z. Wang, and D. Yu, "Cross-lingual knowledge graph alignment via graph matching neural network," in *Conference of the Association for Computational Linguistics (ACL)*, 2019, pp. 3156–3161.
- [6] X. Liu, H. Hong, X. Wang, Z. Chen, E. Kharlamov, Y. Dong, and J. Tang, "Selfkg: Self-supervised entity alignment in knowledge graphs," in *ACM Web Conference (WWW)*, 2022, pp. 860–870.
- [7] Z. Wang, Q. Lv, X. Lan, and Y. Zhang, "Cross-lingual knowledge graph alignment via graph convolutional networks," in *Conference on Empirical Methods in Natural Language Processing (EMNLP)*, 2018, pp. 349–357.
- [8] Z. Sun, C. Wang, W. Hu, M. Chen, J. Dai, W. Zhang, and Y. Qu, "Knowledge graph alignment network with gated multi-hop neighborhood aggregation," in *AAAI Conference on Artificial Intelligence (AAAI)*, vol. 34, no. 01, 2020, pp. 222–229.
- [9] X. Mao, W. Wang, H. Xu, Y. Wu, and M. Lan, "Relational reflection entity alignment," in *ACM International Conference on Information & Knowledge Management (CIKM)*, 2020, pp. 1095–1104.
- [10] X. Mao, W. Wang, H. Xu, M. Lan, and Y. Wu, "Mraea: an efficient and robust entity alignment approach for cross-lingual knowledge graph," in *Proceedings of the 13th International Conference on Web Search and Data Mining (WSDM)*, 2020, pp. 420–428.
- [11] Z. Sun, W. Hu, Q. Zhang, and Y. Qu, "Bootstrapping entity alignment with knowledge graph embedding," in *International Joint Conference on Artificial Intelligence (IJCAI)*, vol. 18, no. 2018, 2018, pp. 4396–4402.
- [12] Z. Zhang, H. Liu, J. Chen, X. Chen, B. Liu, Y. Xiang, and Y. Zheng, "An industry evaluation of embedding-based entity alignment," in *Proceedings of the 28th International Conference on Computational Linguistics: Industry Track*, 2020, pp. 179–189.
- [13] X. Zhao, W. Zeng, J. Tang, W. Wang, and F. M. Suchanek, "An experimental study of state-of-the-art entity alignment approaches," *IEEE Transactions on Knowledge and Data Engineering*, vol. 34, no. 6, pp. 2610–2625, 2020.
- [14] H. Xu, L. Xiang, F. Huang, Y. Weng, R. Xu, X. Wang, and C. Zhou, "Grace: Graph self-distillation and completion to mitigate degree-related biases," in *Proceedings of the 29th ACM SIGKDD Conference on Knowledge Discovery and Data Mining*, 2023, pp. 2813–2824.
- [15] Z. Sun, M. Chen, and W. Hu, "Knowing the no-match: Entity alignment with dangling cases," in *Proceedings of the 59th Annual Meeting of the Association for Computational Linguistics and the 11th International Joint Conference on Natural Language Processing (ACL-IJCNLP)*, 2021, pp. 3582–3593.
- [16] M. Chen, Y. Tian, M. Yang, and C. Zaniolo, "Multilingual knowledge graph embeddings for cross-lingual knowledge alignment," in *Proceedings of the 26th International Joint Conference on Artificial Intelligence (IJCAI)*, 2017, pp. 1511–1517.
- [17] S. Luo, P. Cheng, and S. Yu, "Semi-constraint optimal transport for entity alignment with dangling cases," 2022. [Online]. Available: <https://doi.org/10.48550/arXiv.2203.05744>
- [18] R. Kiryo, G. Niu, M. C. Du Plessis, and M. Sugiyama, "Positive-unlabeled learning with non-negative risk estimator," in *Advances in Neural Information Processing Systems 30: Annual Conference on Neural Information Processing Systems (NIPS)*, 2017, pp. 1675–1685.
- [19] G. Niu, M. C. Du Plessis, T. Sakai, Y. Ma, and M. Sugiyama, "Theoretical comparisons of positive-unlabeled learning against positive-negative learning," in *Advances in Neural Information Processing Systems (NeurIPS)*, 2016, pp. 1199–1207.
- [20] T. N. Kipf and M. Welling, "Semi-supervised classification with graph convolutional networks," 2016. [Online]. Available: <https://arxiv.org/abs/1609.02907>
- [21] Y. Li, J. Chen, Y. Li, Y. Xiang, X. Chen, and H.-T. Zheng, "Vision, deduction and alignment: An empirical study on multi-modal knowledge graph alignment," in *IEEE International Conference on Acoustics, Speech and Signal Processing (ICASSP)*. IEEE, 2023, pp. 1–5.
- [22] Y. Li, Y. Li, X. Chen, H.-T. Zheng, and Y. Shen, "Active relation discovery: Towards general and label-aware open relation extraction," 2023. [Online]. Available: <https://arxiv.org/abs/2211.04215>
- [23] S. Ji, S. Pan, E. Cambria, P. Marttinen, and S. Y. Philip, "A survey on knowledge graphs: Representation, acquisition, and applications," *IEEE Transactions on Neural Networks and Learning Systems (TNNLS)*, vol. 33, no. 2, pp. 494–514, 2021.
- [24] A. Bordes, N. Usunier, A. Garcia-Duran, J. Weston, and O. Yakhnenko, "Translating embeddings for modeling multi-relational data," in *Advances in Neural Information Processing Systems (NeurIPS)*, vol. 26, 2013, pp. 2787–2795.
- [25] Y. Yu, X. Si, C. Hu, and J. Zhang, "A review of recurrent neural networks: Lstm cells and network architectures," *Neural computation*, vol. 31, no. 7, pp. 1235–1270, 2019.
- [26] J. Pennington, R. Socher, and C. D. Manning, "Glove: Global vectors for word representation," in *Conference on Empirical Methods in Natural Language Processing (EMNLP)*, 2014, pp. 1532–1543.
- [27] F. Feng, Y. Yang, D. Cer, N. Arivazhagan, and W. Wang, "Language-agnostic bert sentence embedding," in *Annual Meeting of the Association for Computational Linguistics (ACL)*, 2022, pp. 878–891.
- [28] Y. Gao, X. Liu, J. Wu, T. Li, P. Wang, and L. Chen, "Clusterea: Scalable entity alignment with stochastic training and normalized mini-batch similarities," in *ACM SIGKDD Conference on Knowledge Discovery and Data Mining (SIGKDD)*, 2022, pp. 421–431.
- [29] Z. Liu, Y. Cao, L. Pan, J. Li, and T.-S. Chua, "Exploring and evaluating attributes, values, and structures for entity alignment," in *Conference on Empirical Methods in Natural Language Processing (EMNLP)*, 2020, pp. 6355–6364.
- [30] J. D. M.-W. C. Kenton and L. K. Toutanova, "Bert: Pre-training of deep bidirectional transformers for language understanding," in *Proceedings of NAACL-HLT*, 2019, pp. 4171–4186.
- [31] X. Tang, J. Zhang, B. Chen, Y. Yang, H. Chen, and C. Li, "Bert-int: a bert-based interaction model for knowledge graph alignment," in *Proceedings of the Twenty-Ninth International Conference on International Joint Conferences on Artificial Intelligence*, 2021, pp. 3174–3180.
- [32] Z. Zhong, M. Zhang, J. Fan, and C. Dou, "Semantics driven embedding learning for effective entity alignment," in *2022 IEEE 38th International Conference on Data Engineering (ICDE)*. IEEE, 2022, pp. 2127–2140.
- [33] P. Velickovic, G. Cucurull, A. Casanova, A. Romero, P. Liò, and Y. Bengio, "Graph attention networks," in *6th International Conference on Learning Representations (ICLR)*, 2018.
- [34] Z. Sun, Q. Zhang, W. Hu, C. Wang, M. Chen, F. Akrami, and C. Li, "A benchmarking study of embedding-based entity alignment for knowledge graphs," *Proceedings of the VLDB Endowment*, vol. 13, no. 12, 2020.
- [35] J. Liu, Z. Sun, B. Hooi, Y. Wang, D. Liu, B. Yang, X. Xiao, and M. Chen, "Dangling-aware entity alignment with mixed high-order proximities,"

*Findings of the Association for Computational Linguistics: NAACL 2022*, 2022.

- [36] G. Luo, J. Li, H. Peng, C. Yang, L. Sun, P. S. Yu, and L. He, "Graph entropy guided node embedding dimension selection for graph neural networks," in *Proceedings of the Thirtieth International Joint Conference on Artificial Intelligence, IJCAI*, 2021, pp. 2767–2774.
- [37] A. Surisetty, D. Chaurasiya, N. Kumar, A. Singh, G. Dhama, A. Malhotra, A. Arora, and V. Dey, "Reps: Relation, position and structure aware entity alignment," in *Companion Proceedings of the Web Conference 2022 (WWW)*, 2022, pp. 1083–1091.
- [38] K. Belhajjame and M.-Y. Mejri, "Online maintenance of evolving knowledge graphs with rdfs-based saturation and why-provenance support," *Journal of Web Semantics (JoWS)*, vol. 78, p. 100796, 2023.
- [39] X. Mao, W. Wang, Y. Wu, and M. Lan, "Boosting the speed of entity alignment 10×: Dual attention matching network with normalized hard sample mining," in *Proceedings of the Web Conference 2021 (WWW)*, 2021, pp. 821–832.
- [40] Y. Cao, Z. Liu, C. Li, J. Li, and T.-S. Chua, "Multi-channel graph neural network for entity alignment," in *Proceedings of the 57th Annual Meeting of the Association for Computational Linguistics (ACL)*, 2019, pp. 1452–1461.
- [41] C. Li, Y. Cao, L. Hou, J. Shi, J. Li, and T. Chua, "Semi-supervised entity alignment via joint knowledge embedding model and cross-graph model," in *Proceedings of the 2019 Conference on Empirical Methods in Natural Language Processing and the 9th International Joint Conference on Natural Language Processing, EMNLP-IJCNLP*, 2019, pp. 2723–2732.
- [42] Q. Zhu, X. Zhou, J. Wu, J. Tan, and L. Guo, "Neighborhood-aware attentional representation for multilingual knowledge graphs," in *Proceedings of the Twenty-Eighth International Joint Conference on Artificial Intelligence (IJCAI)*, 2019, pp. 1943–1949.
- [43] H.-W. Yang, Y. Zou, P. Shi, W. Lu, J. Lin, and X. Sun, "Aligning cross-lingual entities with multi-aspect information," in *Proceedings of the 2019 Conference on Empirical Methods in Natural Language Processing and the 9th International Joint Conference on Natural Language Processing (EMNLP-IJCNLP)*, 2019, pp. 4431–4441.
- [44] Y. Wu, X. Liu, Y. Feng, Z. Wang, R. Yan, and D. Zhao, "Relation-aware entity alignment for heterogeneous knowledge graphs," in *Proceedings of the Twenty-Eighth International Joint Conference on Artificial Intelligence*. International Joint Conferences on Artificial Intelligence, 2019.
- [45] R. K. Srivastava, K. Greff, and J. Schmidhuber, "Highway networks," 2015. [Online]. Available: <https://arxiv.org/abs/1505.00387>
- [46] Z. Tan, Y. Zhang, J. Yang, and Y. Yuan, "Contrastive learning is spectral clustering on similarity graph," 2023. [Online]. Available: <https://doi.org/10.48550/arXiv.2303.15103>
- [47] H. V. Assel, T. Espinasse, J. Chiquet, and F. Picard, "A probabilistic graph coupling view of dimension reduction," in *Advances in neural information processing systems (NeurIPS)*, 2022, pp. 10 696–10 708.
- [48] T. Chen, S. Kornblith, M. Norouzi, and G. E. Hinton, "A simple framework for contrastive learning of visual representations," in *International conference on machine learning (ICML)*, 2020, pp. 1597–1607.
- [49] Y. Sun, C. Cheng, Y. Zhang, C. Zhang, L. Zheng, Z. Wang, and Y. Wei, "Circle loss: A unified perspective of pair similarity optimization," in *Proceedings of the IEEE/CVF conference on computer vision and pattern recognition (CVPR)*, 2020, pp. 6398–6407.
- [50] G. Lample, A. Conneau, M. Ranzato, L. Denoyer, and H. Jégou, "Word translation without parallel data," in *International Conference on Learning Representations (ICLR)*, 2018.
- [51] Z. Sun, W. Hu, and C. Li, "Cross-lingual entity alignment via joint attribute-preserving embedding," in *International Semantic Web Conference (ISWC)*, 2017, pp. 628–644.
- [52] S. Auer, C. Bizer, G. Kobilarov, J. Lehmann, R. Cyganiak, and Z. G. Ives, "Dbpedia: A nucleus for a web of open data," in *international semantic web conference (ISWC)*, 2007, pp. 722–735.
- [53] A. T. M. D. A. B. Lindberg, B. L. Humphreys, "The unified medical language system," *Yearbook of medical informatics (Yearb Med Inform)*, vol. 2, no. 1, pp. 41–51, 1993.
- [54] C. Deng, Y. Jia, H. Xu, C. Zhang, J. Tang, L. Fu, W. Zhang, H. Zhang, X. Wang, and C. Zhou, "Gakg: A multimodal geoscience academic knowledge graph," in *Proceedings of the 30th ACM International Conference on Information & Knowledge Management (CIKM)*, 2021, pp. 4445–4454.
- [55] L. Guo, Z. Sun, and W. Hu, "Learning to exploit long-term relational dependencies in knowledge graphs," in *International conference on machine learning (ICML)*, 2019, pp. 2505–2514.
- [56] Z. Sun, J. Huang, W. Hu, M. Chen, L. Guo, and Y. Qu, "Transedge: Translating relation-contextualized embeddings for knowledge graphs," in *The Semantic Web–ISWC 2019: 18th International Semantic Web Conference (ISWC)*, 2019, pp. 612–629.
- [57] K. G. Larsen and J. Nelson, "Optimality of the johnson-lindenstrauss lemma," in *2017 IEEE 58th Annual Symposium on Foundations of Computer Science (FOCS)*, 2017, pp. 633–638.